Murdoch
UNIVERSITY

MURDOCH RESEARCH REPOSITORY

This is the author's final version of the work, as accepted for publication following peer review but without the publisher's layout or pagination. The definitive version is available at
http://dx.doi.org/10.1016/j.nano.2016.02.020

Seydoux, E., Rodriguez-Lorenzo, L., Blom, R.A.M., Stumbles, P.A., Petri-Fink, A., Rothen-Rutishauser, B.M., Blank, F. and von Garnier, C. (2016) Pulmonary delivery of cationic gold nanoparticles boost antigen-specific CD4+ T Cell Proliferation. Nanomedicine: Nanotechnology, Biology and Medicine, 12 (7). pp. 1815-1826.

http://researchrepository.murdoch.edu.au/32281/

Copyright © 2016 Elsevier Inc.

Accepted Manuscript

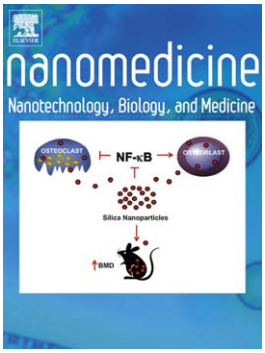

Pulmonary Delivery of Cationic Gold Nanoparticles Boost Antigen-Specific $CD4^+$ T Cell Proliferation

Emilie Seydoux, Laura Rodriguez-Lorenzo, Rebecca A.M. Blom, Philip A. Stumbles, Alke Petri-Fink, Barbara Rothen Rutishauser, Fabian Blank, Christophe von Garnier

PII: S1549-9634(16)30011-9
DOI: doi: 10.1016/j.nano.2016.02.020
Reference: NANO 1308

To appear in: *Nanomedicine: Nanotechnology, Biology, and Medicine*

Received date: 27 October 2015
Revised date: 15 February 2016
Accepted date: 16 February 2016

Please cite this article as: Seydoux Emilie, Rodriguez-Lorenzo Laura, Blom Rebecca A.M., Stumbles Philip A., Petri-Fink Alke, Rutishauser Barbara Rothen, Blank Fabian, von Garnier Christophe, Pulmonary Delivery of Cationic Gold Nanoparticles Boost Antigen-Specific $CD4^+$ T Cell Proliferation, *Nanomedicine: Nanotechnology, Biology, and Medicine* (2016), doi: 10.1016/j.nano.2016.02.020

This is a PDF file of an unedited manuscript that has been accepted for publication. As a service to our customers we are providing this early version of the manuscript. The manuscript will undergo copyediting, typesetting, and review of the resulting proof before it is published in its final form. Please note that during the production process errors may be discovered which could affect the content, and all legal disclaimers that apply to the journal pertain.

ACCEPTED MANUSCRIPT

ORIGINAL RESEARCH

Gold nanoparticle charge modulates T cell proliferation

Pulmonary Delivery of Cationic Gold Nanoparticles Boost Antigen-Specific $CD4^+$ T Cell Proliferation

Emilie Seydoux[1,3], Laura Rodriguez-Lorenzo[2], Rebecca A.M. Blom[1,3], Philip A. Stumbles[4,5], Alke Petri-Fink[2], Barbara Rothen Rutishauser[2], Fabian Blank[1§*], Christophe von Garnier[1§]

[1] Respiratory Medicine, Department of Clinical Research, Bern University Hospital, Berne, Switzerland

[2] Adolphe Merkle Institute, University of Fribourg, Fribourg, Switzerland

[3] Graduate School for Cellular and Biomedical Sciences, University of Berne, Berne, Switzerland

[4] School of Veterinary and Life Sciences, Molecular and Biomedical Sciences, Murdoch University, Perth, Australia

[5] Telethon Kids Institute, Perth, Australia

[§]CvG and FB jointly supervised and contributed equally to this work.

Author contributions:

Conception and design: CvG, FB, ES; Analysis and interpretation: ES, CvG, FB, LR, PS, AF, BR, RB; Planning and execution of experiments: ES, LR, RB; Drafting the manuscript for important intellectual content: ES, FB, CvG, PS, AF, BR;

ACCEPTED MANUSCRIPT

*Corresponding author:

Dr. Fabian Blank

Respiratory Medicine

Department of Clinical Research

Murtenstrasse 50

3008 Berne, Switzerland

Tel: +41 31 632 76 34

Fax +41 31 632 75 94

Email: fabian.blank@dkf.unibe.ch

Complete manuscript word count (incl. body text and figure legends): **4979**

Number of references: **50**

Number of figures: **6**

Number of tables: **1**

Financial and competing interest disclosure

The Swiss National Science Foundation grant NFP64 406440-131266 funded this study. We also acknowledge the support from the Adolphe Merkle Foundation. The authors have no other affiliations or financial involvement with any organization or entity with a financial interest.

ACCEPTED MANUSCRIPT

ACCEPTED MANUSCRIPT

Abstract

To address how surface charge affects the fate of potential nanocarriers in the lung, gold nanoparticles (AuNPs) coated with polyvinyl alcohol containing either positively (NH_2) or negatively (COOH) charged functional groups were intra-nasally instilled in mice, and their uptake by antigen presenting cell populations (APC) in broncho-alveolar lavage (BAL) fluid, trachea, and lung parenchyma, as well as trafficking to the lung draining lymph nodes (LDLNs) was assessed by flow cytometry. Furthermore, $CD4^+$ T cell proliferation in LDLNs was investigated following instillation. All APC subpopulations preferentially captured positively-charged AuNPs compared to their negatively-charged counterparts. Uptake of AuNPs up-regulated expression of co-stimulatory molecules on all APC populations. Furthermore, positively-charged AuNPs induced enhanced OVA-specific $CD4^+$ T cell stimulation in LDLNs compared to negatively-charged AuNPs, or polymer alone. Our findings demonstrate surface charge as a key parameter determining particle uptake by APC, and down-stream immune responses depend on the presence of particle core-bound polymer.

Keywords:

Gold nanoparticles, dendritic cell, macrophage, respiratory tract, immune modulation

ACCEPTED MANUSCRIPT

ACCEPTED MANUSCRIPT

Introduction

The lung is an ideal target organ for needle-free immune modulatory or vaccination approaches given its large surface area endowed by a dense network of antigen-presenting cell populations such as dendritic cells (DCs) and macrophages. Drug delivery through the pulmonary route offers several additional advantages over oral or parenteral delivery due to the presence of a dense vasculature, and a lower concentration of drug-metabolizing enzymes in the lung combined with the highly dispersed nature of an aerosol.[1] Free antigen delivered to the respiratory tract, however, usually fails to induce robust protective effects due to rapid degradation.[2] For these reasons, in recent years, engineered nanomaterials have gained increased interest in the field of innovative biomedical applications. In particular, engineered nanoparticle (NP)-based carrier systems (e.g. mainly NPs with all three dimensions below 100nm (ISO/TS, 2008)) have been proposed as novel therapeutic applications to deliver encapsulated or conjugated molecules of interest (e.g. antigens, allergens, drugs, peptides, proteins, genes, etc.) directly to specific cellular targets, such as antigen-presenting cells (APCs), or more specifically DCs.[3–5] Depending on the degradation rate of the NP-based carrier, such an approach would enable controlled antigen release over time for novel immune-modulatory strategies.[6] To date an increasing number of studies regarding inhalable NP-based carriers is emerging emphasizing the importance of respiratory tract targeting biomedical approaches. For example, recent studies with mice using in particular bio-mimetic nanoparticles demonstrated prolonged persistence, lower inflammatory potential, increased antigen transport to draining lymph nodes, improved specific effector memory T cell responses and significant protection against respiratory challenge infection.[789] In addition, several aerosolized vaccines, such as NP-conjugated to ovalbumin, are being developed and have shown promising first results.[10,11 12]

We and others have shown in the past that NPs not only can serve as carriers, but are also endowed with intrinsic immuno-modulatory properties that may either be required or undesirable for a specific application.[10,13–15] In particular, physicochemical properties, such as size, shape, surface

ACCEPTED MANUSCRIPT

functionalization with different coatings and charges may alter interactions of NPs with immune cells. For instance, we recently reported that intra-nasally administered polystyrene particles with a diameter of 20 nm were more frequently captured by DCs, compared to larger 1000 nm particles, and only the smallest particles led to enhanced antigen-specific $CD4^+$ T cell proliferation in lung draining lymph nodes (LDLNs).[13] Despite an increasing body of literature in the area, little is known on how NP surface chemistry and charge govern interaction with resident APC populations in different respiratory tract compartments upon inhalation.

We hypothesized that NP functionalization with different surface charges, i.e. either positive or negative, on gold core-bound polymer will influence uptake, trafficking to DLNs and induction of down-stream immune responses by respiratory tract APC populations. We utilized gold NPs (AuNPs) coated with functionalized positively-charged (NH_3^+) or negatively-charged (COO^-) polyvinyl alcohol (PVA) polymers, as it was shown that such polymers improve the colloidal stability and biocompatibility of NPs.[16] We evaluated the distribution of both NH_2-PVA and COOH-PVA AuNPs in different respiratory tract compartments after intranasal administration in BALB/c mice, as well as ovalbumin (OVA) uptake, processing and OVA-specific $CD4^+$ T cell proliferation in non-LDLNs and LDLNs by flow cytometry and confocal microscopy.

Methods

Animals

Female BALB/c and DO11.10 TCR transgenic (C.Cg-Tg(DO11.10)10DLo/J) mice were bred specific pathogen free at the Department of Clinical Research (University of Bern, Switzerland) according to the Swiss Federal Veterinary Office guidelines under animal experimentation permission (BE82/12) and used at 8 to 12 weeks of age.

ACCEPTED MANUSCRIPT

Intranasal administration of gold nanoparticles (AuNPs) for uptake and trafficking experiments

NH_2-PVA AuNPs and COOH-PVA AuNPs were synthesized and characterized as previously described with a slight modification in the molecular weight of PVA (Mowiol 4-88 Mw=31000, Calbiochem, EMD Bioscience, Inc. La Jolla, CA, USA) to obtain comparable sizes of both NPs.[16,17] Particle synthesis and intra-nasal instillation is further described in the online supplementary data section.

CFSE-labeled, OVA-specific $CD4^+$ T cell proliferation in naïve animals

Lymph nodes from female DO11.10 mice were collected and $CD4^+$ T cells were isolated using a CD4 negative isolation kit (Dynabeads Untouched Mouse CD4 Cells kit, Invitrogen, Zug, Switzerland). Cells were labeled with carboxyfluorescein succinimidyl ester (CFSE; eBioscience, Vienna, Austria) and 10^7 stained $CD4^+$ T cells per mouse in 200 µl of PBS were intravenously injected. Two days later, AuNPs were administered i.n. as described above, followed by i.n. delivery of 50 µl OVA (Sigma-Aldrich) diluted in PBS (1 mg/ml) 15 min later. Three days later, LDLNs or non-LDLNs (inguinal, axial and gluteal nodes) were collected and labeled for CD4, the DO11.10 TCR (KJ1-26) and CD69 to determine antigen-specific T cell proliferation (CFSE dilution profiles) by flow cytometry. Data was analyzed using the proliferation tool of Flow Jo software (Tree Star, Ashland, OR, USA) and proliferation was expressed as expansion index (EI).

OVA uptake and processing experiments

50 µl of AuNPs (200 µg/ml) or of PBS were administered i.n. in anaesthetized mice, followed 15 min later by 50 µl of OVA-Alexa Fluor 647 (1 mg/ml; Molecular Probes, Lucerne, Switzerland) or by 50 µl of OVA-DQ (1 mg/ml; Molecular Probes) to determine uptake and processing capacity, respectively, by APC populations. Animals were euthanized 2h or 24h after exposure and tissue (trachea, lung parenchyma, DLNs and BAL) was harvested for preparation of single suspension as described above to measure OVA uptake and processing by flow cytometry.

ACCEPTED MANUSCRIPT

Flow cytometry

Unless indicated otherwise, all antibodies were purchased from eBioscience. All stainings were performed strictly on ice. Cells were stained with CD11c-APC, CD11c-PerCP-Cy5.5, CD11b-APC-Cy7, CD11b-FITC, MHC class II-eF450, CD8α-PE, CD40-FITC (BioLegend), CD86-PE-Cy7 (BioLegend), CD4-APC-Cy7, DO11.10 TCR (KJ-126)-PE and CD69-PE-Cy7. Apoptosis and necrosis were measured by means of Annexin-V-FITC and propidium iodide (PI) staining (BioLegend). Relevant isotype control antibodies were employed.

Statistical analysis

All data are presented as mean ±SEM. Data were analyzed by unpaired Student t-test using GraphPad Prism software (La Jolla, CA, USA). Values were considered significantly different with $p<0.05$ (*), $p<0.005$ (**), $p<0.001$ (***).

Results

AuNP characterization

We thoroughly characterized both COOH-PVA and NH_2-PVA AuNPs by assessing the hydrodynamic radius and the polydispersity index (PDI) using dynamic light scattering (DLS), and surface charge through zeta potential measurements of NP suspensions in PBS. COOH-PVA AuNPs were negatively-charged with a zeta potential of -8.2 mV (±1.2 mV) and NH_2-PVA AuNPs were positively-charged with a zeta potential of 7.2 mV (±2 mV) (Table 1). The hydrodynamic diameter for both AuNPs was comprised between 70 nm (PDI 14%) and 90 nm (PDI 23%) (Table 1). Moreover, colloidal stability in water, PBS 1x and RPMI 1640 cell culture medium supplemented with 10% fetal calf serum (FCS) was determined by optical characterization of UV-Vis spectra and detected no aggregation of AuNPs as previously shown.[18] The quantification of endotoxin content in AuNPs was done on a regular basis and has been described in one of our recent publications. All the used AuNPs suspensions showed endotoxin content of less than 0.1EU/mL.[18]

ACCEPTED MANUSCRIPT

Inhaled particle uptake and trafficking by respiratory tract antigen-presenting cells

To analyze APC-dependent particle uptake and trafficking in different respiratory tract compartments, we sampled the BAL (representing the alveolar space), trachea (representing the main conducting airways), lung parenchyma (representing the alveolar tissue), and LDLNs in BALB/c mice 24h after exposure to either to 50 µl PBS (control), 50 µl NH_2-PVA AuNPs or 50 µl COOH-PVA AuNPs for 24h. Organs were sampled 24h after exposure to allow sufficient time for particle trafficking to LDLNs.[13] Control experiments with NH_2-PVA and COOH-PVA polymers were also included in order to distinguish between effects of the polymer-AuNPs and those of the polymer alone. Our gating strategy to identify resident respiratory APC populations includes three different populations (online supplementary data, Figure E1): $CD11c^+$ MHC class II^{low} macrophages, $CD11c^+$ MHC class II^{high} $CD103^-$ $CD11b^+$ DCs ("$CD11b^+$ DCs") and $CD11c^+$ MHC class II^{high} $CD103^+$ $CD11b^-$ DCs ("$CD11b^-$ DCs").[19] In BAL, only $CD11b^+$ DCs were identified. In LDLNs, DC subpopulations were further subdivided into migratory $CD8\alpha^-$ DCs and resident $CD8\alpha^+$ DCs, yielding four final subsets. This gating strategy facilitates analysis of both active cell-dependent transport and passive NP drainage to regional LDLNs.[13,19] The analyses presented herein only include migratory $CD8\alpha^-$ DCs, as no particle-dependent signals were observed in resident $CD8\alpha^+$ DCs (data not shown), indicating that the majority of AuNPs detected in LDLNs are trafficked by cell-mediated transport. Our results showed that macrophages from BAL internalized significantly more NH_2-PVA AuNPs compared to COOH-PVA AuNPs ($p=0.0007$). This was also observed for polymer alone ($p=0.0006$) (Figure 1B). There was no difference between NH_2-PVA AuNPs and NH_2-PVA polymer controls, whereas frequencies of macrophages positive for COOH-PVA AuNPs were significantly higher than those positive for the COOH-PVA polymer alone ($p=0.0095$). A similar trend was observed in the $CD11b^+$ DC sub-population. Significant higher uptake of NH_2-PVA polymer occurred compared to COOH-PVA polymer ($p=0.011$), but differences in uptake did not reach significance between NH_2-PVA AuNPs and COOH-PVA AuNPs ($p=0.09$). Particle and polymer uptake frequency by macrophages and DC subpopulations

ACCEPTED MANUSCRIPT

in trachea was relatively low (<10%) (Figure 1B) with no significant differences seen in macrophages, $CD11b^-$ or $CD11b^+$ DCs positive for NH_2-PVA compared to COOH-PVA AuNPs and polymers. Within the lung parenchyma, macrophages more frequently captured NH_2-PVA AuNPs than COOH-PVA AuNPs ($p=0.013$) and NH_2-PVA polymer compared to COOH-PVA polymer ($p=0.0078$) (Figure 1B). $CD11b^+$ and $CD11b^-$ DCs also captured AuNPs and their respective polymers, albeit to a much lower extent than macrophages (less than 4% of positive cells). Although not significant, there was a trend for more frequent capture of NH_2-PVA AuNPs compared to COOH-PVA AuNPs both by $CD11b^+$ DC ($p=0.1$) and $CD11b^-$ DC subpopulations ($p=0.06$). Low frequencies of particle- or polymer-positive migratory $CD11b^+$ $CD8\alpha^-$ and $CD11b^-$ $CD8\alpha^-$ DCs were detected in LDLNs, with less than 2% of total gated cells (Figure 1B) and no differences seen in trafficking between different particle or polymer types. $CD8\alpha^+$ resident DCs were also analyzed but no particle or polymer-dependent signal was detected for this cell population (data not shown). The amount of AuNPs taken up by different APC subsets in the different lung compartments was also analyzed as measured by mean fluorescence intensity (MFI) (Figure E2). No significant MFI differences were measured between the different APC subsets, with the only exception of BALF macrophages that internalized significantly more NH_2-PVA AuNPs compared to COOH-PVA AuNPs ($p=0.0347$).

OVA-specific $CD4^+$ T cell proliferation after exposure to OVA and AuNPs

We further examined how NH_2-PVA or COOH-PVA AuNPs and respective polymers modulated downstream immune responses by measuring antigen-specific $CD4^+$ T cell proliferation in LDLNs. Following intranasal exposure to OVA/PBS, OVA/NH_2-PVA AuNPs, OVA/NH_2-PVA polymers, OVA/COOH-PVA AuNPs or OVA/COOH-PVA polymers, proliferation was significantly increased in LDLNs compared to non-LDLNs (internal negative-control), in which the EI remained around 1 (Figure 2C). Significantly increased proliferation was observed in mice exposed to OVA/NH_2-PVA AuNPs compared to mice receiving OVA/COOH-PVA AuNPs or OVA/PBS. Proliferation in mice exposed to both OVA/NH_2-PVA polymers and OVA/COOH-PVA polymers was also similar to OVA/PBS exposure

ACCEPTED MANUSCRIPT

(Figure 2C). These results indicate an intrinsic immuno-modulatory effect of intact NH_2-PVA AuNPs but not the NH_2-PVA polymer alone.

Expression of co-stimulatory molecules CD40 and CD86 after the administration of AuNPs or polymers

To understand if the observed increased proliferation following exposure to NH_2-PVA AuNPs was dependent on co-stimulatory molecule expression, we assessed CD40 (Figure 3) and CD86 (Figure 4) expression on $CD11b^+$ DC, $CD11b^-$ DC and macrophage populations in different respiratory tract compartments 24h after AuNP or polymer administration. We observed an overall trend for increased expression of co-stimulatory molecules on particle- or polymer-containing APCs ("AuNP+" in Figures 3 and 4) compared to animals treated with PBS ("PBS" in Figures 3 and 4) or APCs of exposed animals not containing particles or polymers ("AuNP-" in Figures 3 and 4). There was no detectable difference in CD40 and CD86 expression between mice treated with NH_2-PVA AuNPs, COOH-PVA AuNPs or the respective polymers. An exception was seen in BAL, where COOH-PVA polymers induced significantly increased expression of CD40 and CD86 compared to NH_2-PVA polymers in macrophages (CD40; p=0.038) and $CD11b^+$ DCs (CD40; p=0.015, and CD86; p=0.049). No significant difference was observed between AuNP-treated and polymer-treated groups.

OVA uptake and processing after exposure to OVA and AuNPs

We next examined whether NH_2-PVA AuNPs and COOH-PVA AuNPs induced functional changes in APCs by measuring antigen uptake and processing in different respiratory tract compartments. OVA coupled to Alexa Fluor-647 and OVA coupled to DQ were used to analyze antigen uptake and antigen processing, respectively[20]. There was an overall trend for increased OVA uptake after 24h exposure compared to 2h exposure (Figure 5B), but this reached significance only in BAL macrophages ("COOH", p=0.006) and $CD11b^+$ DCs ("NH_2", p=0.011; "COOH", p=0.026), in lung parenchyma macrophages ("COOH", p=0.029) and in LDNLs $CD11b^-$ DCs ("NH_2", p=0.02) (Figure 5B). Similarly,

ACCEPTED MANUSCRIPT

there was an overall trend for enhanced OVA processing in BAL after 24h compared to the 2h time-point (Figure 6, upper panels). In the lung parenchyma, significantly increased antigen processing occurred in $CD11b^+$ DC populations after 24h for both particle types, while in $CD11b^-$ DCs higher antigen processing capacity was present early at 2h compared to the 24h late time-point (only significant for "COOH", p=0.034) (Figure 6, middle panels). Finally, in DC populations, OVA processing in the LDLNs was significantly higher after 24h compared to after 2h (Figure 6, lower panels).

Discussion

Colloidal AuNPs are presently used for labeling, drug delivery, heating and sensing in the biomedical field.[21] For drug delivery, AuNPs offer the advantage that they are straightforward to synthesize, with a core size between 1 nm and 150 nm, can be well colloidally stabilized, biocompatible, and may be functionalized with molecules via thiol-gold bonds.[22] Although numerous *in vivo* studies on the utilization of AuNPs have been performed, e.g. for cell targeting in cancer therapy,[23] there is insufficient knowledge of how inhaled AuNPs distribute in lung tissues, interact with resident immune cells, and whether surface functionalization affects particle-cell interactions.

We aimed to analyze how Au-NP functionalization with two different polymers, NH_2-PVA and COOH-PVA, affected resident APCs and downstream immune responses in the respiratory tract under steady-state conditions. Our data indicated that the majority of AuNPs were captured by macrophages, although low-grade uptake also occurred in $CD11b^+$ and $CD11b^-$ DCs. In BAL and lung parenchyma, APC populations more frequently captured NH_2-PVA AuNPs compared to COOH-PVA AuNPs. Compared to negatively charged COOH-PVA AuNPs or polymers only, we detected enhanced OVA-specific $CD4^+$ T cell stimulation in LDLNs following administration of NH_2-PVA AuNPs that was unrelated to changes in co-stimulatory molecule expression, antigen uptake, or antigen processing in APC populations.

ACCEPTED MANUSCRIPT

One salient finding in our study was that the majority of AuNPs, independently of their surface charge, were taken up by macrophages. Recent studies have emphasized the complex role of pulmonary macrophages in inflammatory processes due to their high level of plasticity and their ability to polarize into a plethora of different phenotypes depending on signals present in the microenvironment,[24,25] which may promote either pro- or anti-inflammatory responses.[26] One of the most important features of respiratory tract macrophages is their distinct phagocytic activity, contributing to tissue homeostasis by the clearance of invading pathogens, debris, as well as apoptotic cells, and preventing inflammatory responses from occurring in order to maintain vital alveolar gas exchange.[27,28] Moreover, uptake by macrophages is non-specific and NPs are likely to be degraded or inactivated.[22] These findings are in line with a study by Geiser and co-workers that evaluated the distribution of 21 nm AuNPs following aerosolization in BAL and lung parenchyma of wild type mice.[29] They observed that 24h after aerosol inhalation, approximately 80% of AuNPs were found within macrophages, while the remaining AuNPs were attached to or within epithelial cells. In another study utilizing a triple cell co-culture model simulating the alveolar lung epithelium, 15 nm AuNPs were found to enter all cell types, i.e. epithelial cells, macrophages and DCs; however a quantification of particles per cell type was not performed.[30] In the present study, a differential uptake between NH_2-PVA and COOH-PVA AuNPs was observed, with amine-functionalized, positively-charged particles preferentially captured by macrophages as compared to carboxylated AuNPs. These results confirm *in vitro* findings from other groups describing an increased uptake of particles with positive charge (e.g. gold, silver, polystyrene, superparamagnetic iron oxide) compared to negatively-charged particles.[16,31–34] Furthermore, a recent *in vivo* study with mice exposed to hydrogel rod-shaped NPs of different surface charge, showed enhanced uptake by AM, CD11b+ DC and CD103+ DC and enhanced trafficking to the LDLNs compared to anionic NPs. The authors of this study therefore suggested that cationic NPs may serve as potential immunomodulators in the lung.[35] Despite the fact that we have instilled an NP dosage 10 fold lower than the dosage used in the study above, we have detected similar effects of positively charged NPs in the respiratory tract and show

ACCEPTED MANUSCRIPT

evidence of a modulated downstream effector T cell response. The effect of positive particle charge may partly be explained by the fact that it favors the adhesion of NPs to the slightly negatively charged cell membrane, although previous studies also showed that the overall charge of both negatively and positively charged NPs in complete medium is similar[34]. Furthermore, the number of dyes per particle was comparable between the two types of NPs (table 1), therefore differences in ATTO590 fluorescent signal in FACS was due to the number of NPs taken up cells rather than due to a difference in the number of dyes on the particles.

We detected relatively lower frequencies of particle-positive $CD11b^+$ and $CD11b^-$ DC subpopulations compared to macrophages. Specifically targeting DCs to increase particle uptake will be the great challenge in the development of novel carriers for vaccines in the respiratory tract and may be achieved by coupling ligands (e.g. antibodies) such as anti-DEC205 or anti-DC-SIGN, on the NP surface for binding to DC surface receptors.[36,37] Similar uptake patterns have already been shown with micro- and nano-sized polystyrene particles intra-nasally instilled in mice.[13,38,39] However, a striking difference in uptake frequency between macrophages and DCs may be explained by the quantity and the location of the cells involved. In particular, located at the luminal side of the alveoli, macrophages represent the first line of defence against deposited pathogens, while DCs, located below the epithelial cells, are present in lower numbers[13,40] and are not directly exposed to but take up deposited particles by extending their dendrites between the epithelial cells into the alveolar lumen as shown by Thornton and co-workers.[41] In our study, the amount of AuNP internalized as measured by MFI analysis, did not differ between DC subsets and AM, indicating similar endocytic activity in lung APC populations analysed.

Our data indicated that there was no difference in particle uptake between $CD11b^+$ and $CD11b^-$ DC subpopulations for both types of AuNPs. A previous *in vivo* study from our group showed that negatively-charged polystyrene NPs of identical diameter (100nm) were captured by both $CD11b^+$ and $CD11b^-$ DC subpopulations to the same extent.[13] Notably, migratory $CD11b^-$ DCs containing 20 nm and 50 nm NPs in LDLNs displayed higher trafficking frequencies compared to migratory $CD11b^+$

ACCEPTED MANUSCRIPT

DCs, which can be explained by the fact that since CD103 belongs to the integrin family and binds to E-cadherin expressed by epithelial cells, $CD11b^-$ DCs are known to be located between epithelial cells and to extend their dendrites between the epithelial layer directly into the airway lumen to sample inhaled antigen deposited in the respiratory tract, allowing to efficiently sample inhaled antigen.[42–44] On the other hand, $CD11b^+$ DCs are expected to be located in the submucosa of the conducting airways and parenchyma without crossing the airway epithelial barrier. Hence, they only sample antigen that has crossed the basal membrane. Moreover, although no charge-dependent particle uptake frequency was seen among different subpopulations of pulmonary DCs, a trend (p=0.06) for higher uptake of NH_2-PVA AuNPs was found in $CD11b^-$ DC from the lung parenchyma when compared to uptake of COOH-PVA AuNPs in this subpopulation. This finding is in line with the results of a recent study, where similar AuNPs were tested by exposing human monocyte-derived DCs *in vitro*.[18]

We detected no charge-dependent differences in frequencies of particle-positive $CD11b^+$ and $CD11b^-$ DCs in LDLNs. Moreover, we did not observe particle-positive resident $CD11b^+$ $CD8\alpha^+$ or $CD11b^-$ $CD8\alpha^+$ DCs after 24h (data not shown), indicating that passive drainage of both NH_2-PVA and COOH-PVA AuNPs to regional lymph nodes did not take place to any measurable extent. These results are in line with a study by Wikstrom and colleagues, which shows that the majority of inhaled antigens detected in the LDLNs is associated with $CD8\alpha^-$ DCs.[45] Also, similar results were found in the study already discussed above, where polystyrene particles of a broad size range from 1000 nm down to 20 nm were mainly found inside $CD8\alpha^-$ DCs.[13] Detection of both types of AuNPs in LDLNs was low with less than 2% of DCs being particle-positive. A possible reason for low detection of AuNPs inside DCs of LDLNs may be due to limited sensitivity of the flow cytometry equipment to detect weak signals of ATTO590 or low total amounts of intra-cellular AuNPs. Quantification of NPs with remarkable sensitivity may be achieved by inductively coupled plasma-optical emission spectroscopy (ICP-OES), a method that can quantify intracellular NPs down to a few picograms, and which was used to quantify similar AuNPs upon uptake by human monocyte-derived DCs *in vitro* as discussed above.[18] Employing

ACCEPTED MANUSCRIPT

this technique for in vivo studies would have required extensive cell-sorting which is beyond the scope of this study.

Monitoring T cell activation after AuNP treatment, we made two salient observations: First, a significantly increased proliferation of antigen-specific $CD4^+$ T cells occurred in animals exposed to co-administered OVA/NH_2-PVA AuNPs as compared to mice that received OVA/PBS or OVA/COOH-PVA AuNPs. Second, NH_2-PVA functionalised AuNPs, but not the NH_2-PVA polymer alone induced an enhanced T cell proliferation. From these two findings three important conclusions may be drawn: **(1)** DC-dependent trafficking of positively-charged NH_2-PVA AuNPs and antigen to LDLNs was sufficient to induce $CD4^+$ T cell stimulation, **(2)** NP surface charge determines downstream T cell activation, and **(3)** the "intact" NP core-polymer hybrid is essential to trigger a downstream immune responses. Our second conclusion harmonizes well with the current literature where, for example, a recent study by Choi and co-workers demonstrated the importance of NP surface charge affecting individual trafficking patterns following instillation into the lungs of rats.[46] Altered particle trafficking to the LDLNs due to particle surface charge may therefore strongly affect downstream immune responses. Supporting our third conclusion, another recent study investigating pro-inflammatory effects of Iron (Fe)- and Au-NP embedded in a poly(methacrylic acid) (PMA) and particle shells alone, also demonstrated altered pro-inflammatory response when coated NPs were compared to shells alone or when different cores (with the same PMA coating) were compared together.[47] To our knowledge the current study is the first description in the field demonstrating that surface charge of NPs alters *in vivo* $CD4^+$ T cell proliferation and that this effect is not restricted to the polymer coating, but requires "intact" NPs with a core-bound polymer shell.

To explain the altered T cell activation with NH_2-PVA modified AuNPs we investigated the effect of AuNPs on activation and function of respiratory tract DCs. We measured the expression of the co-stimulatory surface molecules CD40 and CD86 as markers for DC activation following uptake of AuNPs. The baseline frequency of expression of both CD40 and CD86 was generally increased in both DC- and macrophages that contained particles, independently of the surface charge, except in BAL

ACCEPTED MANUSCRIPT

where COOH-PVA AuNPs and polymers induced a higher expression of CD40 and CD86 compared to their NH_2 equivalents. A possible explanation for the lower frequencies of activated DCs containing NH_2-PVA AuNPs in the BAL may be an increased migration of activated DCs from the alveolar space to LDLNs, where these cells trigger an increased $CD4^+$ T stimulation. In line with the current study, our recent investigation analyzing size-dependent trafficking of different sized polystyrene nanoparticles in the respiratory tract of BALB/c mice also revealed the presence of activated macrophages and DCs ($CD40^{\pm}$, $CD86^{\pm}$) following uptake, independent of particle size.[13] Also, we observed that the potential of DCs to take up and process OVA antigens was also not altered by the exposure to both types of AuNPs, therefore increased $CD4^+$ T cell proliferation cannot be explained by an alteration of DC activation. Furthermore, we measured levels of early apoptosis and necrosis by means of Annexin-V and PI staining in DC and AM populations following exposure to PBS and both types of AuNPs or polymers. Our results showed no significantly increased apoptosis or necrosis any treatment group compared to PBS controls (Figure E3), indicating that the observed effects of NH2-PVA AuNPs are not explained toxicity-related inflammatory responses in the different lung compartments. Other reasons for increased proliferation could be explored, such as altered T cell cytokine secretion profiles[48] or increased adsorption of negatively-charged OVA to positively-charged surface by electrostatic attractive interactions.[49] Moreover, paralleling AuNP uptake, both $CD11b^+$ and $CD11b^-$ DC populations in lung parenchyma take up OVA and traffic to LDNLs to the same extent. These results are consistent with a study by Wikstrom and al. that analyzed OVA uptake in main conducting airways and lung parenchyma, where little difference in OVA uptake by $CD11b^+$ and $CD11b^-$ DCs was observed.[42] OVA processing however, showed a different picture: while processing by $CD11b^+$ DC populations in lung parenchyma increased over time, $CD11b^-$ DCs showed a higher processing capacity after 2h, which then decreases after 24h.[42] Lower amounts of OVA^+ $CD11b^-$ DCs in the lung parenchyma after 24h may be explained by increased trafficking of these cells towards to LDLNs antigen is taken up and processed. In line with these findings, a study by Belz et al. found as well that solely lung $CD11b^-$ DCs were responsible for protein delivery to the LDLNs.[50]

ACCEPTED MANUSCRIPT

In conclusion, this study provides to our knowledge the first evidence that surface charge determines uptake of AuNPs by APC subpopulations in different respiratory tract compartments and is able to modulate downstream $CD4^+$ T cell proliferation in draining lymph nodes. Moreover, the charge-dependent effect was not mediated by the polymer alone, but required an "intact" Au core-bound polymer. These findings have important implications for the future development of innovative NP-based carriers for pulmonary drug delivery and emphasize the importance of painstakingly assessing immune responses of NPs developed for novel clinical applications.

Acknowledgments

We gratefully acknowledge the expert technical assistance provided by Sandra Barnowski and Patrizia Facklam. Microscopy acquisition and analysis were performed with the support of the Live Cell Imaging Core Facility of the Department of Clinical Research coordinated by the Microscopy Imaging Center at the University of Bern, Switzerland.

References

1. Patton JS, Byron PR. Inhaling medicines: delivering drugs to the body through the lungs. *Nat Rev*. 2007;6(1):67–74.
2. Csaba N, Garcia-Fuentes M, Alonso MJ. Nanoparticles for nasal vaccination. *Adv Drug Deliv Rev*. 2009;61(2):140–57.
3. Joshi MD, Unger WJ, Storm G, van Kooyk Y, Mastrobattista E. Targeting tumor antigens to dendritic cells using particulate carriers. *J Control release*. 2012;161(1):25–37.
4. Kunda NK, Somavarapu S, Gordon SB, Hutcheon G a, Saleem IY. Nanocarriers targeting dendritic cells for pulmonary vaccine delivery. *Pharm Res*. 2013;30(2):325–41.
5. Paulis LE, Mandal S, Kreutz M, Figdor CG. Dendritic cell-based nanovaccines for cancer immunotherapy. *Curr Opin Immunol*. 2013;25:1–7.
6. Sung J, Pulliam B, Edwards D. Nanoparticles for drug delivery to the lungs. *TRENDS Biotechnol*.

ACCEPTED MANUSCRIPT

2007;25(12):563–570.

7. Ross KA, Haughney SL, Petersen LK, Boggiatto P, Wannemuehler MJ, Narasimhan B. Lung Deposition and Cellular Uptake Behavior of Pathogen-Mimicking Nanovaccines in the First 48 Hours. *Adv Healthc Mater*. 2014;3(7):1071–1077. doi:10.1002/adhm.201300525.
8. Li A V, Moon JJ, Abraham W, et al. Generation of effector memory T cell-based mucosal and systemic immunity with pulmonary nanoparticle vaccination. *Sci Transl Med*. 2013;5(204):204ra130. doi:10.1126/scitranslmed.3006516.
9. Mann JFS, McKay PF, Arokiasamy S, Patel RK, Klein K, Shattock RJ. Pulmonary delivery of DNA vaccine constructs using deacylated PEI elicits immune responses and protects against viral challenge infection. *J Control Release*. 2013;170(3):452–459. doi:10.1016/j.jconrel.2013.06.004.
10. Nembrini C, Stano A, Dane KY, et al. Nanoparticle conjugation of antigen enhances cytotoxic T-cell responses in pulmonary vaccination. *PNAS*. 2011;108(44):E989–97.
11. Blank F, Stumbles P, von Garnier C. Opportunities and challenges of the pulmonary route for vaccination. *Expert Opin Drug Deliv*. 2011;8(5):547–63.
12. Taratula O, Kuzmov A, Shah M, Garbuzenko O, Minko T. Nanostructured lipid carriers as multifunctional nanomedicine platform for pulmonary co-delivery of anticancer drugs and siRNA. *J Control Release*. 2013;171(3):349–57.
13. Blank F, Stumbles PA, Seydoux E, et al. Size-dependent Uptake of Particles by Pulmonary APC Populations and Trafficking to Regional Lymph Nodes. *Am J Respir Cell Mol Biol*. 2013;49:67–77.
14. Blank F, Gerber P, Rothen-Rutishauser B, et al. Biomedical nanoparticles modulate specific CD4(+) T cell stimulation by inhibition of antigen processing in dendritic cells. *Nanotoxicology*. 2011;5:606–21.
15. Hardy CL, LeMasurier JS, Belz GT, et al. Inert 50-nm polystyrene nanoparticles that modify pulmonary dendritic cell function and inhibit allergic airway inflammation. *J Immunol*. 2012;188(3):1431–41.
16. Rodriguez-Lorenzo L, Fytianos K, Blank F, von Garnier C, Rothen-Rutishauser B, Petri-Fink A. Fluorescence-Encoded Gold Nanoparticles: Library Design and Modulation of Cellular Uptake into Dendritic Cells. *Small*. 2014:1–10.
17. Enüstün B, Turkevich J. Coagulation of colloidal gold. *J Am Chem Soc*. 1963;85(21).
18. Fytianos K, Rodriguez-Lorenzo L, Clift MJD, et al. Uptake efficiency of surface modified gold nanoparticles does not correlate with functional changes and cytokine secretion in human dendritic

ACCEPTED MANUSCRIPT

cells in vitro. *Nanomedicine*. 2015;11(3):633–44.

19. Von Garnier C, Filgueira L, Wikstrom M, et al. Anatomical location determines the distribution and function of dendritic cells and other APCs in the respiratory tract. *J Immunol*. 2005;175(3):1609–18.
20. Seydoux E, Rothen-Rutishauser B, Nita IM, et al. Size-dependent accumulation of particles in lysosomes modulates dendritic cell function through impaired antigen degradation. *Int J Nanomedicine*. 2014;9:3885–902.
21. Sperling RA, Rivera Gil P, Zhang F, Zanella M, Parak WJ. Biological applications of gold nanoparticles. *Chem Soc Rev*. 2008;37:1896–1908.
22. Ghosh P, Han G, De M, Kim CK, Rotello VM. Gold nanoparticles in delivery applications. *Adv Drug Deliv Rev*. 2008;60(11):1307–15.
23. Almeida JPM, Figueroa ER, Drezek RA. Gold nanoparticle mediated cancer immunotherapy. *Nanomedicine*. 2014;10(3):503–14.
24. Mosser DM, Edwards JP. Exploring the full spectrum of macrophage activation. *Nat Rev Immunol*. 2008;8(12):958–69.
25. Xue J, Schmidt S V, Sander J, et al. Transcriptome-based network analysis reveals a spectrum model of human macrophage activation. *Immunity*. 2014;40(2):274–88.
26. Robbe P, Draijer C, Borg TR, et al. Distinct macrophage phenotypes in allergic and nonallergic lung inflammation. *Am J Physiol Lung Cell Mol Physiol*. 2015;308(4):L358–67.
27. Hussell T, Bell TJ. Alveolar macrophages: plasticity in a tissue-specific context. *Nat Rev Immunol*. 2014;14(2):81–93.
28. Kirby AC, Coles MC, Kaye PM. Alveolar macrophages transport pathogens to lung draining lymph nodes. *J Immunol*. 2009;183(3):1983–9.
29. Geiser M, Quaile O, Wenk A, et al. Cellular uptake and localization of inhaled gold nanoparticles in lungs of mice with chronic obstructive pulmonary disease. *Part Fibre Toxicol*. 2013;10:1–10.
30. Brandenberger C, Rothen-Rutishauser B, Mühlfeld C, et al. Effects and uptake of gold nanoparticles deposited at the air-liquid interface of a human epithelial airway model. *Toxicol Appl Pharmacol*. 2010;242(1):56–65.
31. Harush-Frenkel O, Rozentur E, Benita S, Altschuler Y. Surface charge of nanoparticles determines their endocytic and transcytotic pathway in polarized MDCK cells. *Biomacromolecules*. 2008;9(2):435–43.

ACCEPTED MANUSCRIPT

doi:10.1021/bm700535p.

32. Marquis BJ, Liu Z, Braun KL, Haynes CL. Investigation of noble metal nanoparticle ζ-potential effects on single-cell exocytosis function in vitro with carbon-fiber microelectrode amperometry. *Analyst*. 2011;136(17):3478–86.

33. Fröhlich E. The role of surface charge in cellular uptake and cytotoxicity of medical nanoparticles. *Int J Nanomedicine*. 2012;7:5577–91. doi:10.2147/IJN.S36111.

34. Hirsch V, Kinnear C, Moniatte M, Rothen-Rutishauser B, Clift MJD, Fink A. Surface charge of polymer coated SPIONs influences the serum protein adsorption, colloidal stability and subsequent cell interaction in vitro. *Nanoscale*. 2013.

35. Fromen CA, Rahhal TB, Robbins GR, et al. Nanoparticle Surface Charge Impacts Distribution, Uptake and Lymph Node Trafficking by Pulmonary Antigen-Presenting Cells. *Nanomedicine Nanotechnology, Biol Med*. 2015. doi:10.1016/j.nano.2015.11.002.

36. Gieseler RK, Marquitan G, Hahn MJ, et al. DC-SIGN-specific liposomal targeting and selective intracellular compound delivery to human myeloid dendritic cells: implications for HIV disease. *Scand J Immunol*. 2004;59(5):415–24.

37. van Broekhoven CL, Parish CR, Demangel C, Britton WJ, Altin JG. Targeting Dendritic Cells with Antigen-Containing Liposomes: A Highly Effective Procedure for Induction of Antitumor Immunity and for Tumor Immunotherapy. *Cancer Res*. 2004;64:4357–4365.

38. Jakubzick C, Tacke F, Llodra J, van Rooijen N, Randolph GJ. Modulation of dendritic cell trafficking to and from the airways. *J Immunol*. 2006;176(6):3578–84.

39. Hardy CL, Lemasurier JS, Mohamud R, et al. Differential uptake of nanoparticles and microparticles by pulmonary APC subsets induces discrete immunological imprints. *J immunol*. 2013;191(10):5278–90.

40. Von Garnier C, Wikstrom ME, Zosky G, et al. Allergic airways disease develops after an increase in allergen capture and processing in the airway mucosa. *J Immunol*. 2007;179(9):5748–59.

41. Thornton EE, Looney MR, Bose O, et al. Spatiotemporally separated antigen uptake by alveolar dendritic cells and airway presentation to T cells in the lung. *J Exp Med*. 2012;209(6):1183–1199. doi:Doi 10.1084/Jem.20112667.

42. Wikstrom ME, Stumbles P a. Mouse respiratory tract dendritic cell subsets and the immunological fate of inhaled antigens. *Immunol Cell Biol*. 2007;85(3):182–8.

ACCEPTED MANUSCRIPT

43. Von Garnier C, Nicod LP. Immunology taught by lung dendritic cells. *Swiss Med Wkly*. 2009;139(13-14):186–92.

44. Holt PG, Strickland DH, Wikström ME, Jahnsen FL. Regulation of immunological homeostasis in the respiratory tract. *Nat Rev Immunol*. 2008;8(2):142–52.

45. Wikstrom ME, Batanero E, Smith M, et al. Influence of mucosal adjuvants on antigen passage and CD4+ T cell activation during the primary response to airborne allergen. *J Immunol*. 2006;177(2):913–24.

46. Choi HS, Ashitate Y, Lee JH, et al. Rapid translocation of nanoparticles from the lung airspaces to the body. *Nat Biotechnol*. 2010;28(12):1300–3.

47. Lehmann AD, Parak WJ, Zhang F, et al. Fluorescent-magnetic hybrid nanoparticles induce a dose-dependent increase in proinflammatory response in lung cells in vitro correlated with intracellular localization. *Small*. 2010;6(6):753–62.

48. Fröhlich E. Value of phagocyte function screening for immunotoxicity of nanoparticles in vivo. *Int J Nanomedicine*. 2015:3761–3778.

49. van der Maaden K, Yu H, Sliedregt K, et al. Nanolayered chemical modification of silicon surfaces with ionizable surface groups for pH-triggered protein adsorption and release: application to microneedles. *J Mater Chem*. 2013:4466–4477.

50. Belz GT, Smith CM, Kleinert L, et al. Distinct migrating and nonmigrating dendritic cell populations are involved in MHC class I-restricted antigen presentation after lung infection with virus. *PNAS*. 2004;101(23):1–6.

ACCEPTED MANUSCRIPT

ACCEPTED MANUSCRIPT

Tables

Hetero-functionalized AuNPs	Hydrodynamic diameter [nm] (Polydispersity)	Zeta Potential [mV] (SD)	Number of dye molecules per particle
COOH-PVA	70 (14 %)	-8.2 (1.2)	717 ± 199
NH_2-PVA	90 (23 %)	7.2 (2.0)	568 ± 144

Table 1. Hydrodynamic diameter, zeta potential and number of dye molecules per particle of ATTO590-conjugated carboxylic-PVA-functionalized (COOH-PVA) and amine-PVA-functionalized (NH_2-PVA) gold NPs (AuNPs).

ACCEPTED MANUSCRIPT

ACCEPTED MANUSCRIPT

Figure legends

Figure 1. Quantification of AuNP uptake by APC Populations using flow cytometry

AuNP or polymer uptake was measured 24h after exposure **(A)**. Gating strategy is described in the online supplementary data (Figure E1). Within each APC population cells positive for particles and polymers were determined with PBS-exposed animals serving as a control. Results show uptake frequencies of NH_2-PVA AuNPs (white bars, left), NH_2-PVA polymers (white bars, right), COOH-PVA AuNPs (black bars, left) and COOH-PVA polymers (black bars, right) by APC populations **(B)**. Results are expressed as Δ positive cells = measured frequency in particle-exposed animals minus measured frequency in PBS-exposed animals. Y-axes have been scaled differently to illustrate differences between groups. Bars show mean ±SEM; *p<0.05, **p<0.005, ***p<0.001 (without bar indication: between NH_2 and COOH); n=6 independent experiments.

Figure 2. Antigen-specific $CD4^+$ T cell proliferation in lung draining lymph nodes (LDLNs) and non-draining lymph nodes (non-DLNs) following intranasal exposure to OVA and AuNPs, polymers or PBS

(**A**) Seventy two hours after administration, $CD4^+$ $DO11.10^+$ T cell proliferation in non-DLNs (internal negative control) and LDLNs was assessed by flow cytometry. (**B**) Gating strategy included a FSC and SSC gating followed by a $CD4^+$ $DO11.10^+$ gating. Histograms of CFSE profiles in non-DLNs (left) and LDLNs (right) were analyzed in order to obtain the expansion index (EI). (**C**) EI values for $CD4^+$ $DO11.10^+$ T cells in non-DLNs (left) and LDLNs (right) after exposure to PBS (white), NH_2-PVA AuNPs (grey), NH_2-PVA polymers (grey), COOH-PVA AuNPs (black) or COOH-PVA polymers (black). Bars show mean ±SEM; *p<0.05, ***p<0.001; n=5 independent experiments.

Figure 3. CD40 expression in APC populations following particle exposure measured by flow cytometry

ACCEPTED MANUSCRIPT

Expression of CD40 was determined 24h after administration in particle-positive ("AuNP+") and particle-negative ("AuNP-") cell populations within the same animal and compared to PBS-exposed animals ("PBS"). Results are expressed as Δ frequency = measured sample frequency minus measured isotype control frequency. White bars: PBS; light grey bars: NH_2-PVA AuNPs; striped light grey bars: NH_2-PVA polymers; dark grey bars: COOH-PVA AuNPs; striped dark grey bars: COOH-PVA polymers. Bars show mean ±SEM; *p<0.05, **p<0.005, ***p<0.001; n=5 independent experiments.

Figure 4. CD86 expression in APC populations following particle exposure measured by flow cytometry

Expression of CD86 was determined 24h after administration in particle-positive ("AuNP+") and particle-negative ("AuNP-") cell populations within the same animal and was compared to PBS-exposed animals ("PBS"). Results are expressed as Δ frequency = measured sample frequency minus measured isotype control frequency. White bars: PBS; light grey bars: NH_2-PVA AuNPs; striped light grey bars: NH_2-PVA polymers; dark grey bars: COOH-PVA AuNPs; striped dark grey bars: COOH-PVA polymers. Bars show mean ±SEM; *p<0.05, **p<0.005 (without bar indication: between AuNP- and AuNP+); n=5 independent experiments.

Figure 5. Antigen uptake by APC populations following exposure to PBS or AuNPs

(A) Mice were administrated intra-nasally PBS only ("ctrl"), PBS + OVA-Alexa Fluor647 ("PBS"), NH_2-PVA AuNPs + OVA-Alexa Fluor647 ("NH_2") or COOH-PVA AuNPs + OVA-Alexa Fluor647 ("COOH"), prior to measuring OVA uptake flow cytometry. **(B**) Results show uptake after 2 hours (white) and 24 hours (black) by APC populations in BAL, lung parenchyma and LDLNs. Results are expressed as mean fluorescence intensity. Y-axes have been scaled differently to illustrate differences between groups. Bars show mean ±SEM; *p<0.05, **p<0.005; n=5 independent experiments.

Figure 6. OVA processing by APC populations following exposure to PBS or AuNPs

ACCEPTED MANUSCRIPT

Mice were administrated intra-nasally PBS only ("ctrl"), PBS + DQ-OVA ("PBS"), NH_2-PVA AuNPs + DQ-OVA ("NH_2") or COOH-PVA AuNPs + DQ-OVA ("COOH"). Results show processing after 2 hours (white) and 24 hours (black) by APC populations in BAL, lung parenchyma and LDLNs. Results are expressed as mean fluorescence intensity. Y-axes have been scaled differently to illustrate differences between groups. Bars show mean ±SEM; *p<0.05, **p<0.005, ***p<0.001; n=5 independent experiments.

ACCEPTED MANUSCRIPT

ACCEPTED MANUSCRIPT

Figures

Figure 1

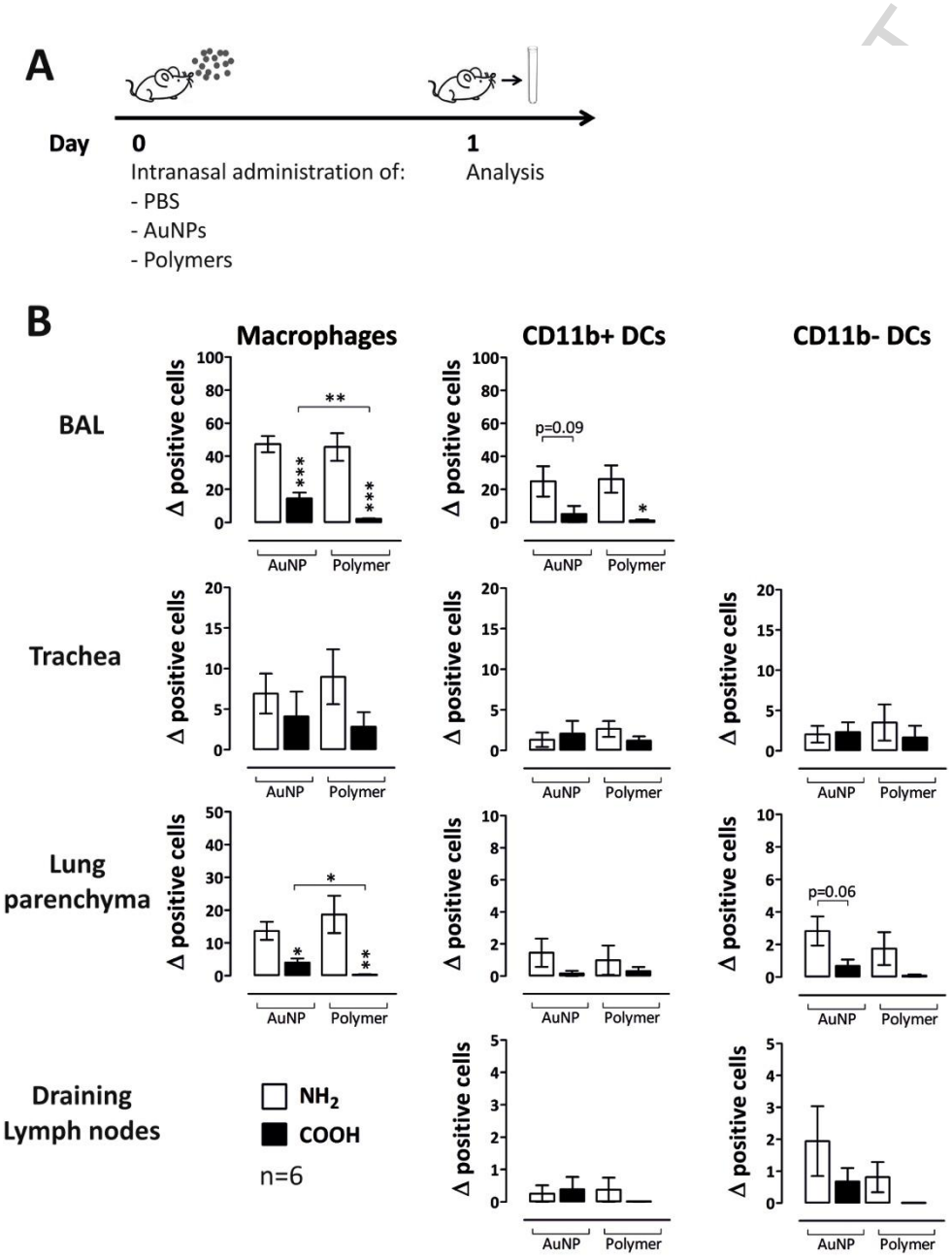

ACCEPTED MANUSCRIPT

Figure 2

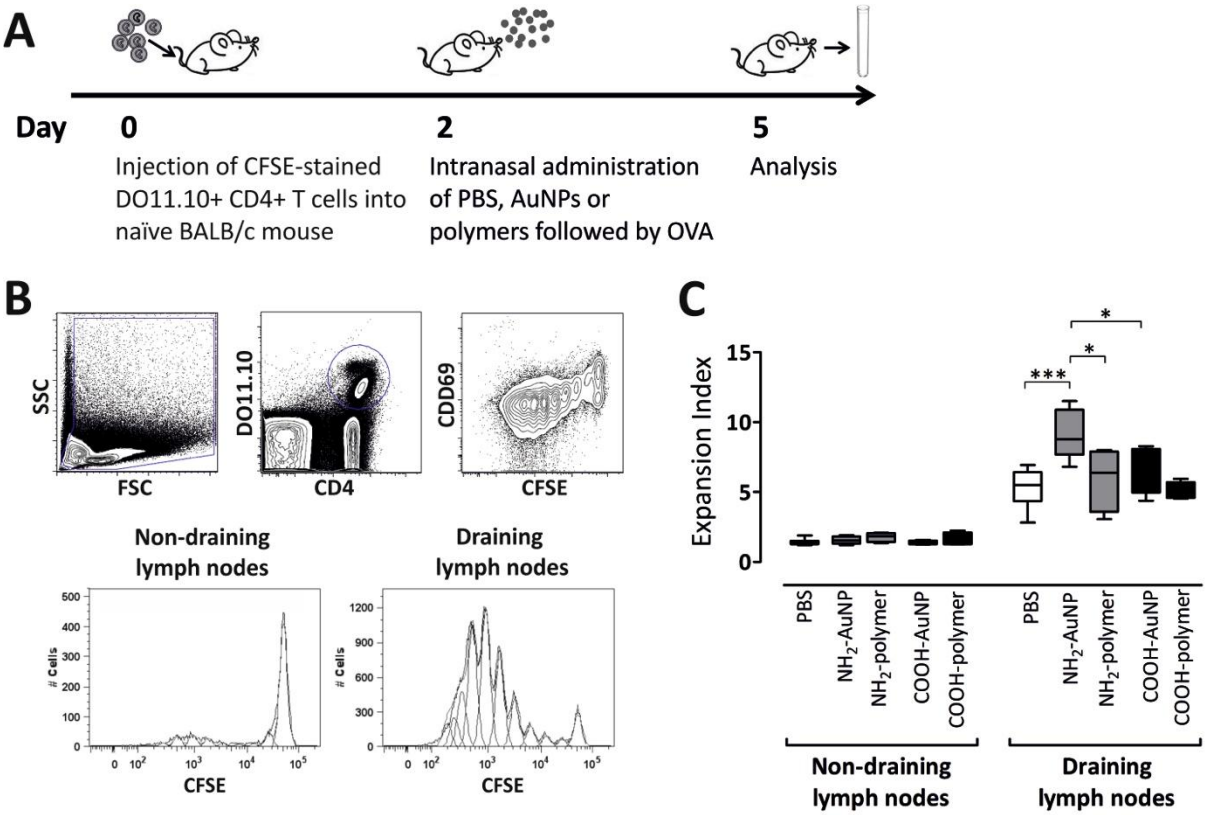

ACCEPTED

ACCEPTED MANUSCRIPT

Figure 3

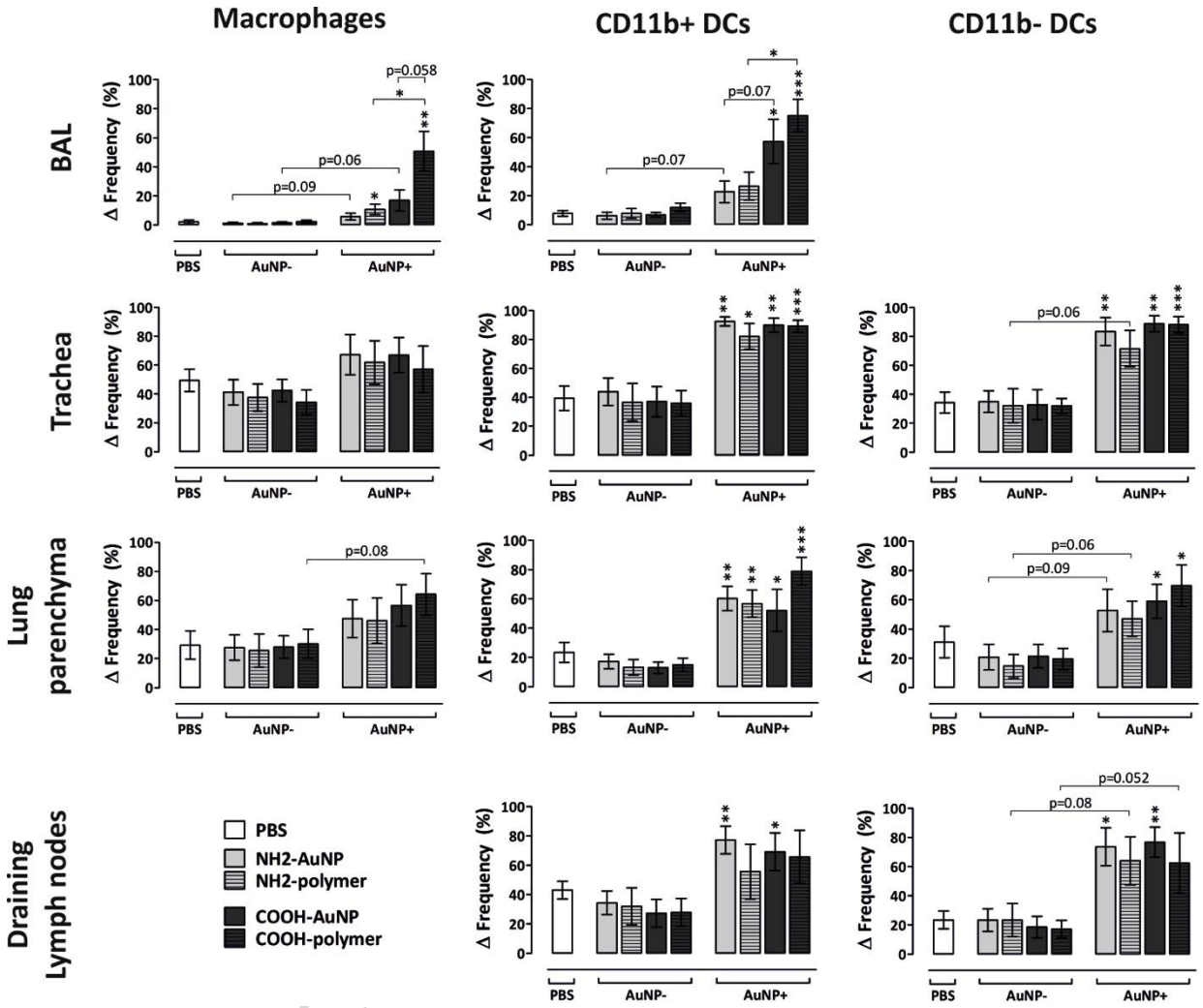

ACC

ACCEPTED MANUSCRIPT

Figure 4

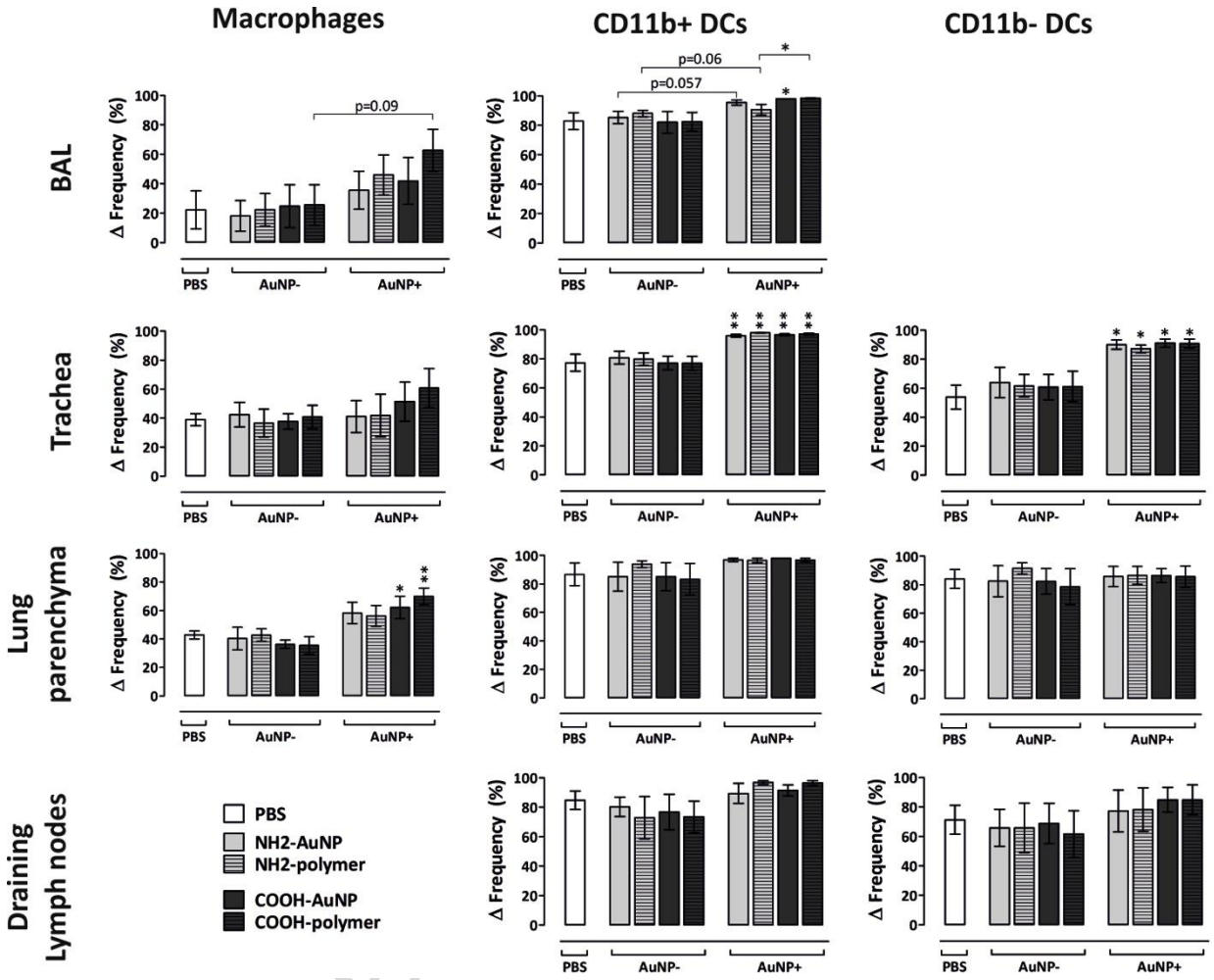

ACCE

ACCEPTED MANUSCRIPT

Figure 5

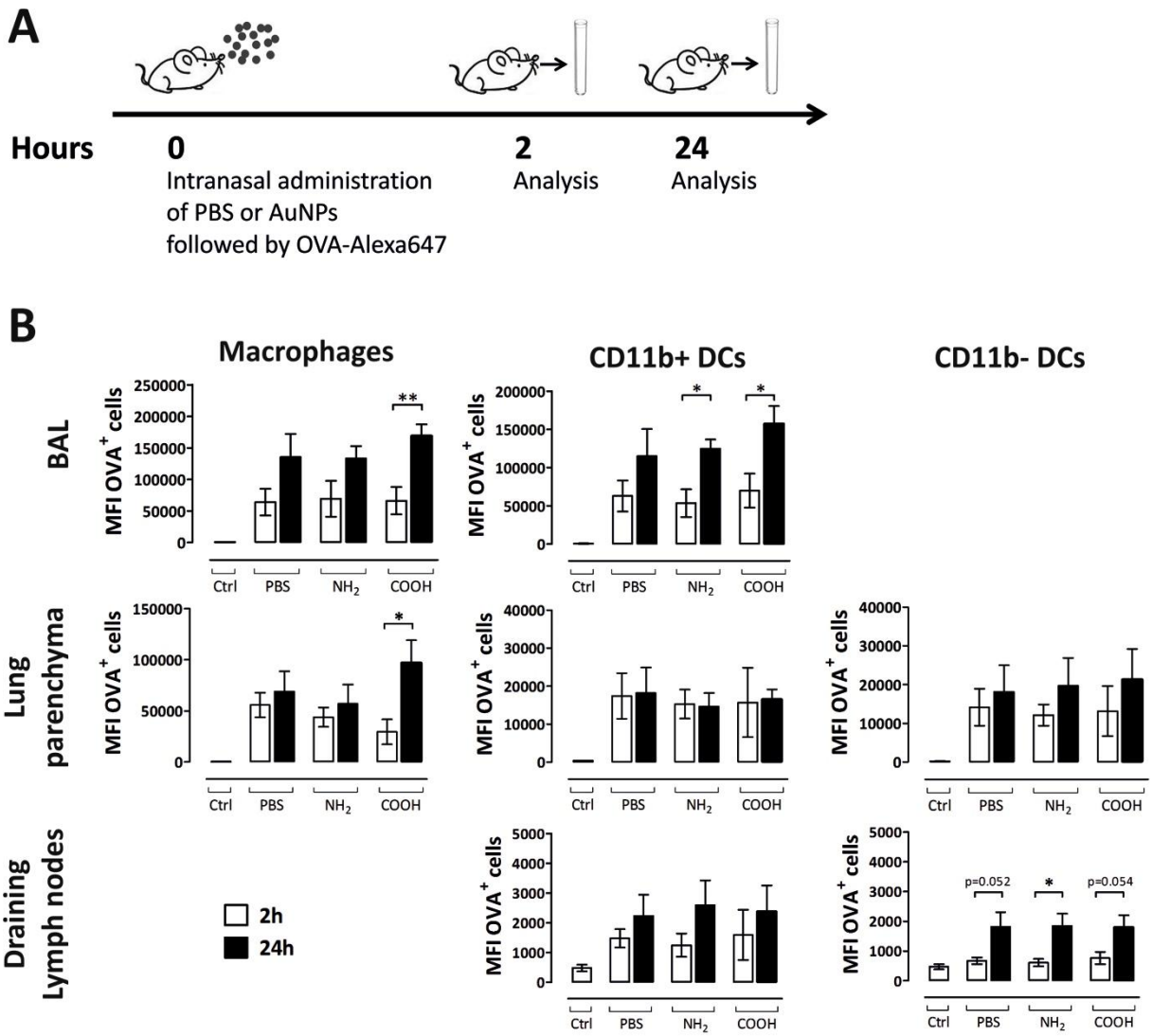

ACCEPTED MANUSCRIPT

Figure 6

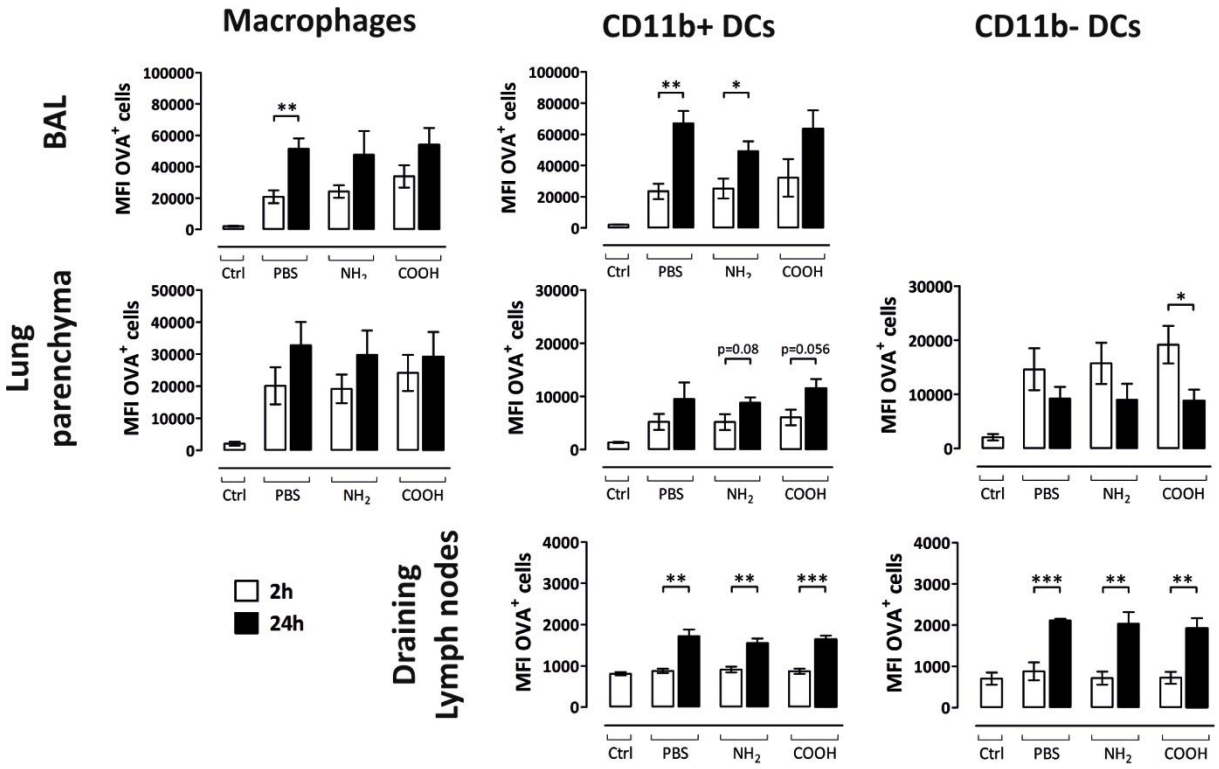

ACCEPTED

ACCEPTED MANUSCRIPT

Graphical Abstract

CD4+ T cell proliferation in lung draining lymph nodes was measured after intra nasal instillation of positively (NH2) charged and negatively charged (COOH) gold nanoparticles or polymer shells alone followed by ovalbumin in a mouse model of ovalbumin induced experimental allergic airways disease (upper panel). Positively charged gold nanoparticles induced enhanced ovalbumin specific T cell proliferation compared to controls (non-exposed), negatively charged gold nanoparticles or positively charged polymer alone (lower panel). This and other findings of the present study highlight the importance of surface charge of a biomedical nanoparticle in modulating a specific adaptive immune response.